Hypoxia activates cells in the pathway from the paraventricular nucleus (PVN) to nucleus tractus solitarii (nTS) in the brainstem

College of Veterinary Medicine, University of Missouri

Elizabeth F. Palmieri, Brian C. Ruyle, K. Max Coldren, Cheryl M. Heesch, and Eileen M. Hasser

College of Veterinary Medicine and Dalton Cardiovascular Research Center, University of Missouri, Columbia, MO 65211

INTRODUCTION

Arterial chemoreceptors sense blood oxygen and send afferent information to the nucleus tractus solitarii (nTS) in the brainstem to elicit ventilatory and cardiovascular responses. The primary pathway contributing to chemoreflex responses involves activation of nTS neurons that project to the rostral ventrolateral medulla (RVLM) to increase respiration, sympathetic nerve activity, and blood pressure. The nTS also projects to the paraventricular nucleus (PVN), a highly integrative region of the hypothalamus which has neuroendocrine, autonomic, and cardiorespiratory functions. Our group has previously shown that PVN-projecting nTS neurons are activated by hypoxia (King et al., 2012), suggesting that the PVN is also an important component of the chemoreflex. Furthermore, previous studies have shown that lesion or inhibition of the PVN blunts cardiorespiratory responses to hypoxia. However, the neural pathways by which the PVN contributes to cardiorespiratory responses to hypoxia are unknown.

The PVN sends efferent projections to brainstem regions involved in cardiovascular and respiratory regulation, including the RVLM, intermediolateral (IML), and the caudal ventrolateral medulla (CVLM). Interestingly, our group has shown that PVN neurons that project to the RVLM or the IML are not activated by hypoxia (Coldren et al, 2013, 2014). In addition, preliminary data suggest PVN neurons projecting to the CVLM are not activated by hypoxia. The PVN sends direct efferent projections back to the nTS. However, the PVN to nTS output has not been studied to specifically determine whether it participates in the hypoxic response.

The PVN is comprised of heterogeneous subpopulations of neurons. Magnocellular PVN neurons produce oxytocin (Oxy) and vasopressin (AVP) and contribute to neuroendocrine regulation of lactation, blood volume, and blood pressure. Previous studies have shown that a subset of nTS-projecting neurons display Oxy- and AVP-immunoreactivity (IR). The parvocellular PVN contributes to both neuroendocrine and autonomic regulation. Parvocellular PVN neurons that synthesize corticotropin releasing hormone (CRH) are involved in the classic neuroendocrine stress response; however, some evidence suggests that CRH may help regulate autonomic output. The magnocellular and parvocellular regions of the PVN contain neuronal nitric oxide synthase (nNOS)-IR neurons that produce nitric oxide (NO). Blockade of NO synthesis in the PVN increases chemoreflex-mediated sympathoexcitation. This suggests that NO in the PVN may modulate sympathetic and ventilatory responses following chemoreflex activation. Our group has previously shown that both nNOS-IR and CRH-IR PVN neurons are activated by hypoxia (Coldren et al., 2013, 2014). Due to the contributions of these PVN phenotypes in autonomic regulation, we investigated their potential involvement in the PVN-nTS pathway in the chemoreflex response to hypoxia.

Immunohistochemistry (IHC) was used to determine the phenotypes of PVN neurons. Specifically, CRH-, nNOS-, Oxy-, and AVP-IR cells were studied. Fos, a protein expressed when cells are acutely activated, was used to study the activation of the PVN by hypoxia. Cholera toxin B (CtB) conjugated to a fluorophore, was injected into the nTS to retrogradely label nTS-projecting PVN cells. Hypoxic activation and the phenotypes of the nTS-projecting cells was assessed.

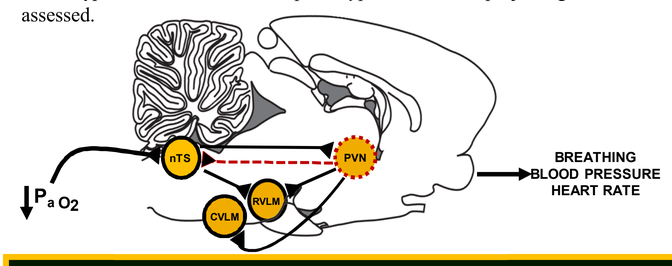

HYPOTHESES

- **nTS-projecting PVN neurons are activated by hypoxia**
- **The phenotype of activated nTS-projecting PVN neurons includes CRH-, nNOS-, Oxy-, and AVP-IR neurons**

METHODS

Animals: Male Sprague Dawley rats (250-350g) were used.

nTS Microinjection: Anesthetized rats were placed in a stereotaxic apparatus, and the brainstem was exposed. Glass micropipettes were placed in the nTS (coordinates for microinjections were 0.4 mm lateral, 0.5 mm ventral from calamus scriptorius) and the retrograde tracer, CtB (1%, conjugated to AlexaFluor (AF) 555), was injected bilaterally (30 nl). Rats were allowed 7-10 days to recover.

Hypoxia Exposure: Following recovery from microinjection surgery, conscious rats were acclimated for 2 hours to a hypoxic chamber (Biospherix) on 3 days at room air prior to the experiment. On the day of the experiment, conscious rats were exposed to either normoxic (21% O_2, n=4) or hypoxic (10% O_2, n = 5) conditions for 2 hrs.

Tissue Preparation: Following normoxic or hypoxic exposure, rats were deeply anesthetized (5% Isoflurane) and transcardially perfused with oxygenated, heparinized Dulbecco's Modified Eagle Medium (DMEM, Sigma) followed by 200-400 ml 4% paraformaldehyde (PFA). Forebrain and hindbrain sections (30 microns) containing the PVN and nTS, respectively, were cut using a vibrating Microtome (VT 1000s; Leica, Germany).

Injection Site Verification: Hindbrain sections containing the nTS were viewed using an epifluorescent Olympus BX51 microscope. Both fluorescent and brightfield (BF) images were taken in order to visualize the retrograde tracer in the nTS. The two images were then superimposed and the location of the center of the injection site was determined using a standard atlas for the rat brain (Paxinos and Watson, 6th edition). Animals were included in the study if the center of the injection site was contained within the nTS, and if retrograde tracer from the nTS region displayed labeling in appropriate regions of the PVN.

Immunohistochemistry (IHC): Free floating forebrain sections were processed for Fos-IR (Rabbit anti-Fos, 1:3000), CRH-IR (Guinea pig anti-CRH, 1:1000), nNOS-IR (Goat anti-nNOS, 1:2000), Oxy-IR (Mouse anti-oxytocin, 1:2000), and AVP-IR (Guinea pig anti-vasopressin, 1:5000). Donkey AF647 anti-rabbit IgG, Donkey AF488 anti-guinea pig IgG, Donkey AMCA anti-goat IgG and Donkey Cy2 anti-mouse IgG were fluorescent secondary antibodies used to visualize the primary antibodies. nTS-projecting cells were identified by the intrinsic fluorescence of the retrograde tracer.

Quantitative Analysis: Four rostral-caudal sections containing the PVN (as defined in Fig 1. below) were viewed using an epifluorescent Olympus BX51 microscope. Images in the same plane were taken using appropriate filter sets, and positively-labeled cells were counted using ImageJ software. PVN neurons that were positive for CtB, Fos-IR, CRH-IR, nNOS-IR, Oxy-IR, and/or AVP-IR were counted unilaterally. **NOTE: In all representative pseudocolored sections, *Fos is RED*, *CRH is GREEN*, *nNOS is BLUE*, *AVP is CYAN*, *Oxy is YELLOW*, *and nTS-projecting is WHITE*.**

nTS injection sites and rostral-caudal PVN levels

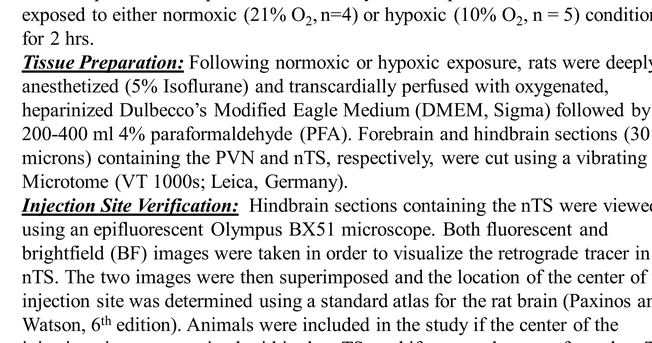

Fig 1. Verification of bilateral nTS injections and PVN levels
A. Epifluorescent photomicrograph of a coronal section of the nTS showing representative injection sites of retrograde tracer. **B.-E.** Outlined regions of the PVN showing presence of cells labeled with retrograde tracer at each of the four rostral-caudal levels. **B.** Level 1 (most rostral)= Bregma -1.6 mm. **C.** Level 2= Bregma -1.8 mm. **D.** Level 3= Bregma -2.1 mm. **E.** Level 4 (most caudal)= Bregma -2.3 mm. CC, central canal; DMX, dorsal motor nucleus of the vagus, TS, tractus solitarius; 3V, third ventricle.

RESULTS

PVN neurons project to the nTS

A. Rostral-caudal distributions of identified PVN neurons

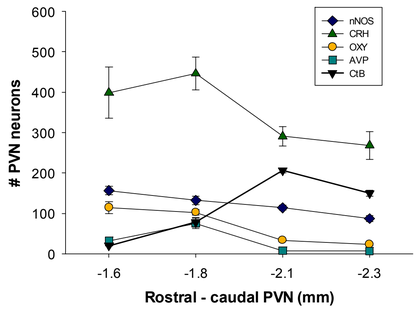

B. Phenotypes of nTS-projecting neurons

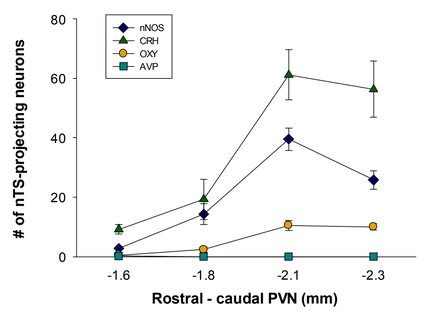

C. Percent of each phenotype that projects to the nTS

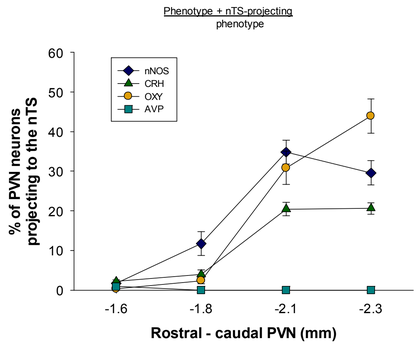

D. Percent of nTS-projecting PVN neurons of a given phenotype

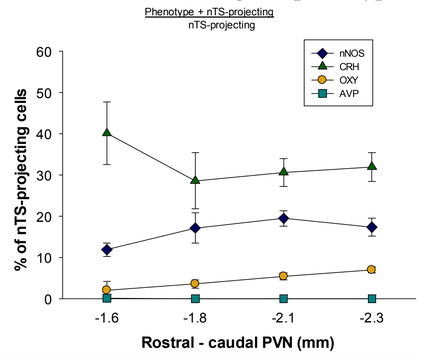

Fig 2. PVN neurons project to the nTS. **A.** Rostral-caudal distribution of nTS-projecting PVN neurons (CtB) and specific PVN phenotypes (CRH-, nNOS-, Oxy-, and AVP-IR cells) across four PVN levels. These phenotypes were not different between the hypoxic and normoxic groups. nTS-projecting neurons (or CtB cells) were highest in number in the caudal two levels of the PVN. CRH-IR cells were highest in number and were localized primarily in the two rostral levels. nNOS- and Oxy-IR cells also were present primarily the rostral PVN. AVP-IR cells were in highest concentration in the mid-rostral PVN (level 2). **B.** The highest number of cells that projected to the nTS were CRH- and nNOS-IR cells-especially in the caudal two levels. Oxy-IR cells minimally projected and AVP-IR projecting cells were negligible. **C.** Of the phenotypes, the highest percent that projected to the nTS were Oxy-, nNOS-, and CRH-IR cells, primarily in the caudal PVN. **D.** Rostral-caudal distribution of nTS-projecting cells of a given phenotype. Very few nTS-projecting PVN neurons were Oxy- or AVP-IR. The highest percentage of nTS-projecting PVN cells were CRH- and nNOS-IR.

Hypoxia activates nTS-projecting PVN neurons

A. Number of activated PVN neurons

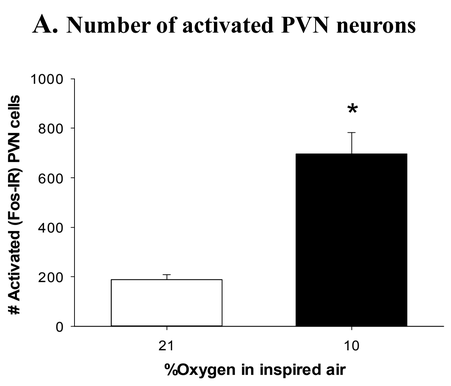

B. Rostral-caudal distribution of activated PVN neurons

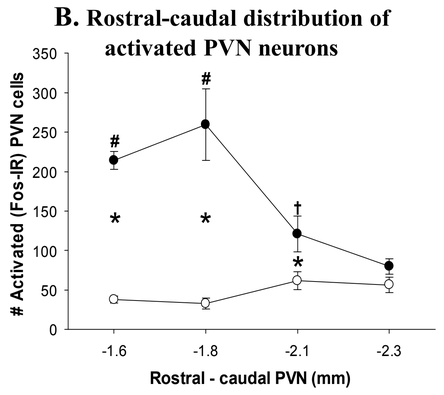

C. Percent of nTS-projecting cells activated by hypoxia

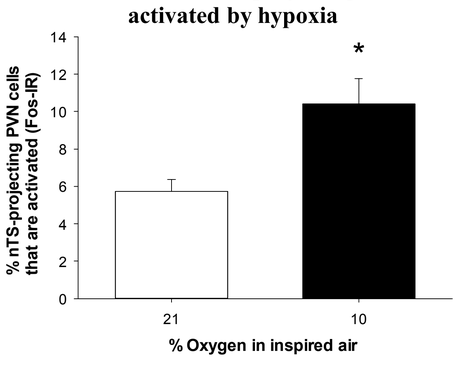

D. Rostral caudal distribution of projecting cells activated by hypoxia

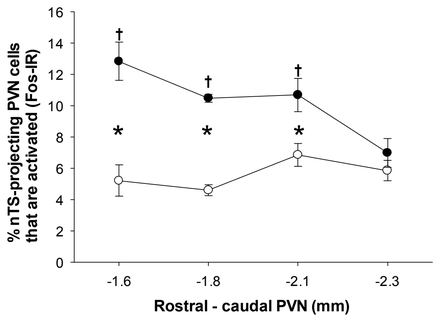

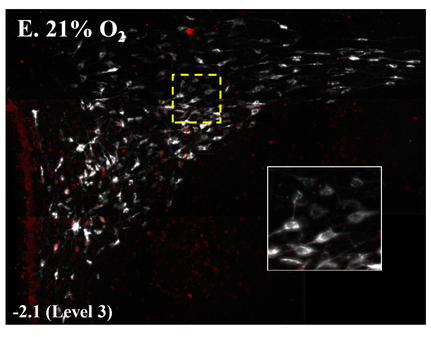

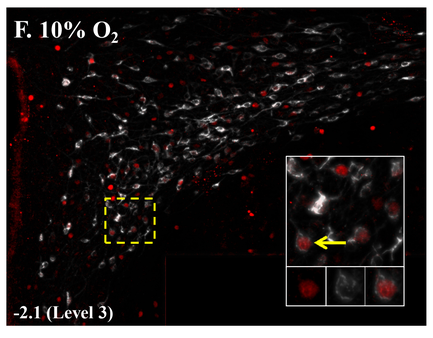

Fig 3. Hypoxia activates nTS-projecting PVN neurons. **A.** Two hours of hypoxia increased the number of Fos-IR cells in the PVN. **B.** Two hours of hypoxia increased the number of Fos-IR neurons primarily in more rostral regions of the PVN. **C.** A higher percentage of nTS-projecting PVN cells showed Fos-IR following two hours of hypoxia versus normoxia. **D.** The percent of nTS-projecting PVN neurons activated following two hours of hypoxia versus normoxia was greatest in more rostral regions of the PVN. **E., F.** Merged photomicrographs of the PVN showing Fos-IR (red) and nTS-projecting (white) cells following normoxia and hypoxia, respectively. For all graphs, * $P \leq 0.05$, 21% vs 10% O_2; # $P \leq 0.05$ vs -2.1 and -2.3; † $P \leq 0.05$ vs -2.3.

CRH- and nNOS-IR nTS-projecting PVN neurons are activated by hypoxia

A. Percent of identified phenotypes activated by hypoxia

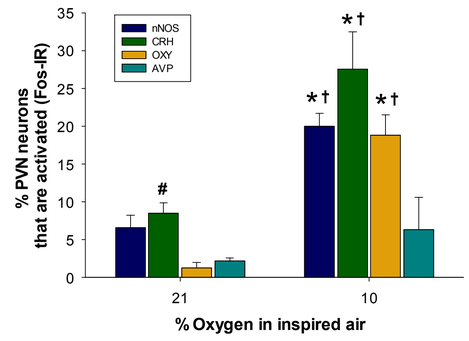

B. Percent of nTS-projecting phenotypes activated by hypoxia

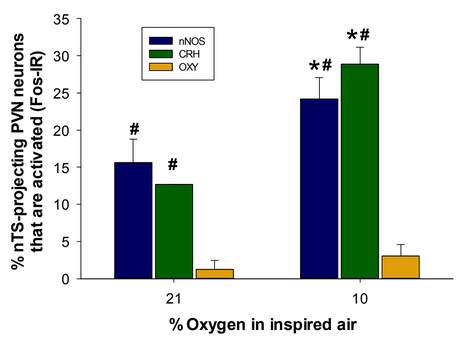

C. Percent of nNOS-IR nTS-projecting cells activated by hypoxia

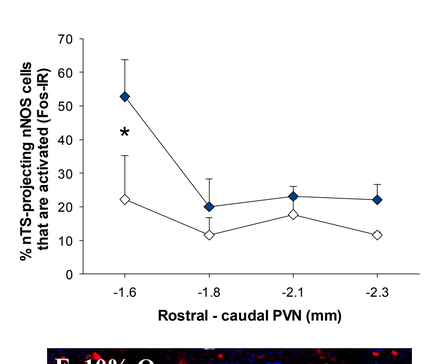

D. Percent of CRH-IR nTS-projecting cells activated by hypoxia

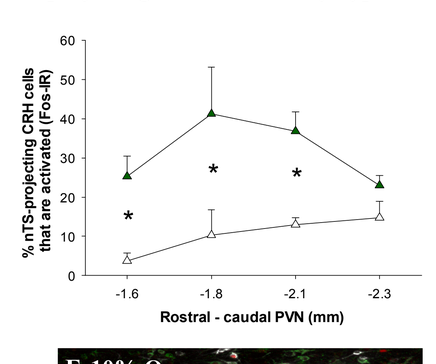

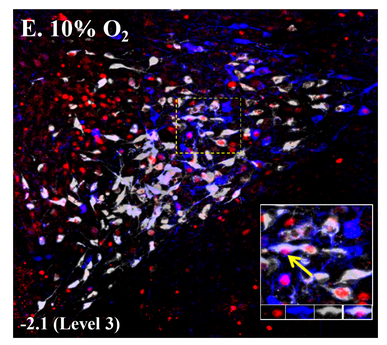

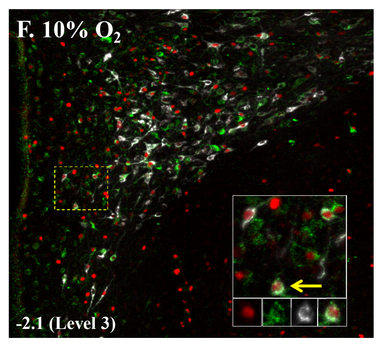

Fig 4. CRH- and nNOS-IR PVN neurons are both activated by hypoxia and project to the nTS. **A.** A greater percentage of CRH-, nNOS-, and Oxy-IR cells were activated (exhibited Fos-IR) following two hours of hypoxia versus normoxia. AVP- IR cells were not significantly activated by two hours of hypoxia. **B.** A greater percent of nTS-projecting nNOS- and CRH-IR cells were activated by hypoxia. Oxy-IR cells that projected were not significantly activated by hypoxia and no AVP-IR cells both projected and were activated (not shown). **C.** The highest percentage of nNOS-IR cells that projected to the nTS were in the most rostral PVN level. **D.** The highest percentage of nTS-projecting CRH-IR cells that were activated by hypoxia were in the rostral and mid-PVN. **E.** Merged photomicrograph of the PVN showing Fos-IR (red), nNOS-IR (blue), and nTS-projecting (white) cells. **F.** Merged photomicrograph of the caudal PVN showing Fos-IR (red), CRH-IR (green), and nTS-projecting (white) cells. For all graphs, * $P \leq 0.05$, 21% vs 10% O_2; # $P \leq 0.05$ vs Oxy and AVP; † $P \leq 0.05$ vs Oxy.

SUMMARY, CONCLUSIONS and FUTURE DIRECTIONS

Summary:

- **Hypoxia activated the PVN shown by an increase in Fos-IR after two hours of hypoxia versus normoxia**
  - **These neurons were found in the rostral PVN**
- **Hypoxia activated PVN neurons that projected to the nTS**
  - **A higher percentage of activated nTS-projecting neurons were found in the rostral PVN**
- **Of the phenotypes examined in the PVN (CRH-, nNOS-, Oxy-, and AVP-IR), nTS-projecting PVN neurons were primarily CRH- and nNOS-IR**
- **Hypoxia activated CRH-, nNOS-, and Oxy-IR neurons in the PVN. AVP-IR neurons were minimally activated**
- **Hypoxia activated nTS-projecting CRH- and nNOS-IR neurons**

Conclusions:

These data suggest that:

- **The PVN projections to the nTS play a role in the chemoreflex response to hypoxia**
- **CRH- and nNOS-IR neurons may play a role in the chemoreflex response to hypoxia in part via the PVN to nTS pathway**

Future Directions:

- **Examine the activation of nTS-projecting PVN neurons that display both nNOS- and CRH-IR**
  - **Determine the extent to which these cells are activated by hypoxia (Fig 5. quadruple-labeled cells)**
- **Analyze the different regions in the PVN among the four levels**
- **Investigate whether the PVN's role in the chemoreflex is by activating nTS neurons that project to the RVLM**
- **Determine what is expressed at the terminals in the nTS from the PVN**

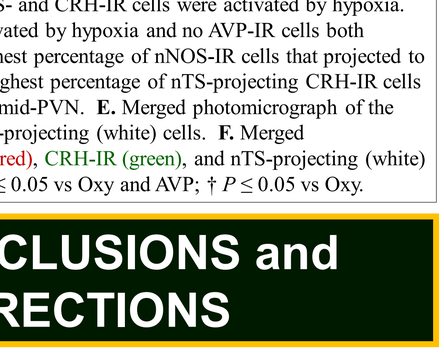

Fig 5. Hypoxia activates nTS-projecting PVN neurons expressing both CRH- and nNOS-IR. Merged photomicrograph of the PVN showing Fos-IR (red), CRH-IR (green), nNOS-IR (blue), and nTS-projecting (white) cells. Quadruple-labeled cells indicate an activated nTS-projecting cell displays both CRH- and nNOS-IR.

Acknowledgements: Funded by NIH and IDEXX-Bioresearch
We thank Sarah A. Friskey for her outstanding technical expertise

References

King, TL, Heesch CM, Clark CG, Kline DD, Hasser EM. Hypoxia activates nucleus tractus solitarii neurons projecting to the paraventricular nucleus of the hypothalamus Am J Physiol 302: R1219-R1232, 2012.

Coldren, KM, McCalmon, SP, King, TL, Kline, DD, Hasser, EM, Heesch, CM. Acute hypoxia (AH) increases Fos-IR in nNOS and AVP cells in the paraventricular nucleus of the hypothalamus (PVN). FASEB J: 27:697.26, 2013.

Coldren, KM, Berka, CM, Kline DD, Hasser, EM, Heesch, CM. Corticotropin releasing hormone neurons in the paraventricular nucleus of the hypothalamus colabeled with nNOS are activated by acute hypoxia. FASEB J:28: 710.8, 2014.